Journal Name

ARTICLE TYPE

π-Conjugation-Interrupted Hyperbranched Polymer Electrets for Organic Nonvolatile Transistor Memory Devices

Jinyi Lin,[a] Wen Li,[a] Zhenzhen Yu,[b] Mingdong Yi,*[a] Haifeng Ling,[a] Linghai Xie,*[a] Shengbiao Li,[b] Wei
5 **Huang*[c, a]**

By means of the limited conjugation length, the intrinsic 3-dimensional conformations and the potential
10 nanoporous structures, π-conjugation-interrupted hyperbranced polymers (CIHPs) were demonstrated as
polymer electrets for the application of organic transistor memory. As models of CIHPs, PPF and PPF8
were synthesized via Friedel-Crafts C-H polymerization for the investigation of structure-performance
relationship according to four-element theory. They exhibited good solubility in organic solvents,
excellent thermal stability and film-forming ability. The preliminary as-fabricated transistors showed the
15 memory effects with the large hysteresis windows and reliable programming/erasing cycles.
Furthermore, devices based on PPF exhibited higher mobility, larger ON/OFF ratio and better data
retention capability than those based on PPF8. The negative effect of the substitution of alkoxyl groups
on the device performance suggest that charge trapping and storage are highly sensitive with electrets'
molecular orbital energy levels, vibration relaxation mode, chain aggregates, and surface energy.
20 Soluble organic framework polymers will be potential advanced organic nanomaterials for plastic
electronics and mechatronics.

Introduction

Organic memory devices have received much attention owing to the advantages of large area, light weight, mechanical flexibility,
25 and low-cost fabrication.[1-9] In the field of organic memories, transistor-type memories are easily integrated into conventional chips with the advantage of good repeatability, non-destructive readout and multibit storage.[10-19] In general, electrical memory effects in the transistors arose from either charge trapping in
30 polymer electrets[20-26] or polarization in ferroelectric materials.[27, 28] In general, ferroelectric polymers have the drawback of the low solubility and high crystallization temperature, polymer electrets become an alternative to achieving high-performance transistor memories.[29, 30] The most polymer electrets were reported to be
35 liner vinyl polymers used in transistor memory by Liu[14, 15] Chen,[16] and Kim.[30] Chen *et. al.* employed a liner polystyrene electret that was para-substituted with a π-conjugated oligofluorene[31] or star-shape polymer.[23, 32] However, up to date, the reported liner or star-shape polymer electrets exhibited
40 unsatisfactory thermal stability with relative low glass transitions temperature (T_g) (< 150 °C),[23, 30, 31] which is unfavourable for the device stability and life time.[33] They also designed the stable polyimides (PIs) electrets that exhibited multi-step synthesis, hydrophilic and polarity properties.[29,34] Thus, it is of great
45 significance to explore polymer electrets with high thermal

stability and excellent solubility via concise synthetic methods.

On the other hand, it is key issue to get sight into the effect of molecular structure on charge trapping in transistor memory in order to make rational molecular design of polymer electrets.
50 many efforts have been made to investigate the effect of molecular structure, such as molecular polarity, conjugated length, and steric interaction, on the electrical memory. Kim *et. al.* demonstrated that hydrophobic and non-polar polymers had memory characteristics superior to those of hydrophilic and polar
55 polymers in pentacene-based transistor memory devices using a series of vinyl polymers as electrets.[21, 30] Besides, the intrinsic nonplanar conformations, topological structures and appropriate conjugation length in polymer electrets are favourable for the charge trapping capability to produce an large threshold shift and
60 well-defined conductance levels for data storage.[23, 35, 36] In addition, the donor-acceptor (*p-n*) polymers enable also enhance the charge storages through the induced intramolecular charge transfer (ICT) from the *p*-type to *n*-type moiety under an applied electric field.[29] The steric hindrance in the *p-n* systems as
65 modified layer between pentacene and electrets can improve the charge trapping at nano-interface, charge mobility and memory window.[37] In a word, it is significant to design new-concept polymer electrets for high-performance organic transistor memories.
70 Polymer semiconductors can be designed in terms of the

electronic structure, steric hindrance, conformation and topology as well as supramolecular interaction that have be extracted into four-element theory.[38,2] Herein, we demonstrated the four-element principle for the design of polymer electrets. In our previous work, we have developed Friedel-Crafts (F-C) reaction of fluorenols at room temperature to synthesize complex diaryfluorenes (CDAFs) with nonplanar conformations,[39-41] and F-C click post-functionalization (FCCP) of polymer semiconductors to construct nonvolatile flash memorable organic materials.[4] We also first developed F-C C-H bond polymerization to synthesize one kind of diarylfluorene-based π-conjugation-interrupted polymers with the feature of congested conformations.[42] In this work, we first reported π-conjugation-interrupted hyperbranched polymer (CIHPs) serving as electrets in pentacene-based transistor memory devices. In contrary to liner polymers, CIHPs exhibited the limited conjugation length, 3-dimensional frameworks, and abundant conformation isomers owing to the introduction of tetrahedral sp^3 hybridized carbon atoms in polymer backbones. Two CIHPs, PPF and PPF8, were designed as model electrets that were synthesized via Lewis acid F-C C-H polymerization. They exhibits the excellent film-forming ability and thermal stability. PPF-based transistor memory device enables the reversible trapping of electron carriers in gate dielectrics. The PPF8 are also prepared to explore the effect of hydrophilic property, topological structure and alkoxyl-substitution on the performance of transistor memory. To the best of our knowledge, this is the first study on transistor memory devices using fluorene-based conjugation-interrupted polymer electrets.

Results and discussion

Synthesis and Thermal Stability of PPF and PPF8. Synthetic routes of the target PPF and PPF8 are depicted in Scheme S1. Fluorenyl tertiary alcohols have high reactivity for F-C reactions according to literatures.[40] Phenyl-fluoren-9-ol (PFOH) and 9-(4-(octyloxy)phenyl)-fluoren-9-ol (PF8OH) can serve as monomers to generate PPF and PPF8 via the CF$_3$SO$_3$H mediated F-C polymerization. Model experiments (I) and (II) were carried out in order to clarify the linking position of monomers in PPF and PPF8. The mainly product in the F-C reaction of fluorenol monomers (PFOH) with 1,4-diethoxybenzene indicated that active site was D site rather than A in PF8OH. However, for the PFOH, the A site was the more active than the site at B, C according to the product of reaction II. Therefore, the polymer structures of PPF and PPF8 were confirmed as showed in Figure 1a. Meanwhile, according to the NMR analysis, the number of H atom at site A was the same as to those of the site at D in d-toluene (Figure S4), further confirmed the structure of PPF8 in Scheme S1 (III) (Figure S1).

For the 3-dimensional structures, although there is no flexible substituent in PPF, both PPF and PPF8 were exhibited excellent solubility in common organic solvents such as chloroform, tetrahydrofuran (THF), and toluene, chlorobenzene. The number-average molecular weight (M_n) and polydispersity index (PDI) of PPF and PPF8, as determined by GPC against a PS standard in THF, were around 6846 and 2.86, and 8687 and 2.62. Differential scanning calorimetry (DSC) and thermo gravimetric analyzer (TGA) were performed for the evaluation of thermal property of

PPF and PPF8 (Figure S2). The results suggested that PPF8 and PPF exhibited outstanding thermal stability, with the decomposition temperature (T_d) (5% weight loss) of 384 and 412 °C. PPF8 also showed excellent morphological stability with distinct T_g appeared at 180 °C, but no distinct transition was observed in DSC traces of PPF recording from 30 to 250 °C. The excellent thermal stability of PPF and PPF8 may attribute to the rigid 3-dimensional network structures hindering the crystallization process of the polymers, which is greatly favourable for the stable polymer electrets in transistor memory devices.
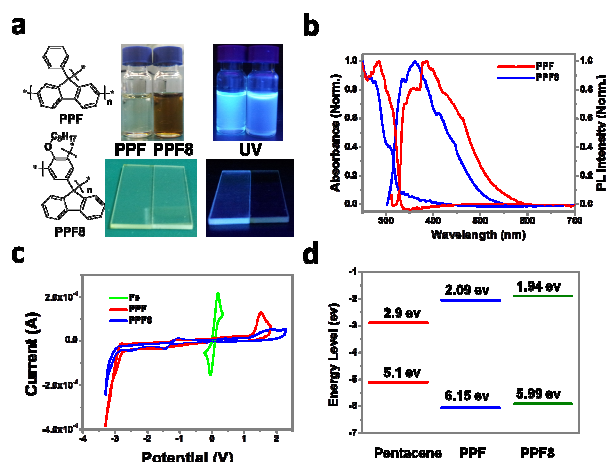
Figure 1. UV-*vis* absorption and PL spectra of PPF and PPF8 films spin-coating from toluene solution (10 mg/ml).

Photophysical Properties of PPF and PPF8. The UV-*vis* absorption and fluorescence analysis of PPF and PPF8 are used to investigate the aggregation behaviour in solution and films (Figure 2, S3 and S4). Transparent thin films were prepared *via* spin-coating from the toluene solutions on quartz plates. In the UV-*vis* absorption spectra of the film, the PPF shows a profiles with the two absorption band at 278 and 310 nm, similar to that of PPF8, which can be assigned to π-π* transition of benzene and the fluorene, respectively.[7] On the other hand, PPF and PPF8 in diluted toluene solution exhibited emission spectra with peaks at 334 and 346 nm, which are consistent with their limited effective conjugation length with wide bandgaps owing to the conjugation-interrupted conformations (Figure S3 and S4). With the increase of concentration, the excimer or aggregation emission at 380-500 nm both found in the emission spectra of PPF and PPF8 films. And the PL spectra of their films showed broader emission peaks at 340, 360, 414 nm for PPF8 and 358, 385, 442 for PPF, which exhibited broader and new shoulders and/or tailing peaks with respect to that in solution, suggesting that intrachain partial overlaps of fluorene groups in the film of PPF and PPF8.[42] Noted that PPF presented more Stoke shifts than PPF8, suggested stronger aggregation and packing of fluorene groups in the films. And it also indicated that the flexible alkoxyl groups in PPF8 would suppress the molecular aggregation. These strong molecular aggregation and well-packed fluorene conformation of CIHPs would useful to afford more trapped charges of transistor memory.[11, 23] Cyclic voltammetry (CV) study shows the highest occupied molecular orbital (HOMO) and lowest unoccupied

molecular orbital (LUMO) energy levels of PPF and PPF8 are -2.09, -6.15 eV and -1.94, -5.99 eV, respectively (Figure 1c and 1d). In this context, alkoxyl substitution would increase the HOMO and LUMO level.
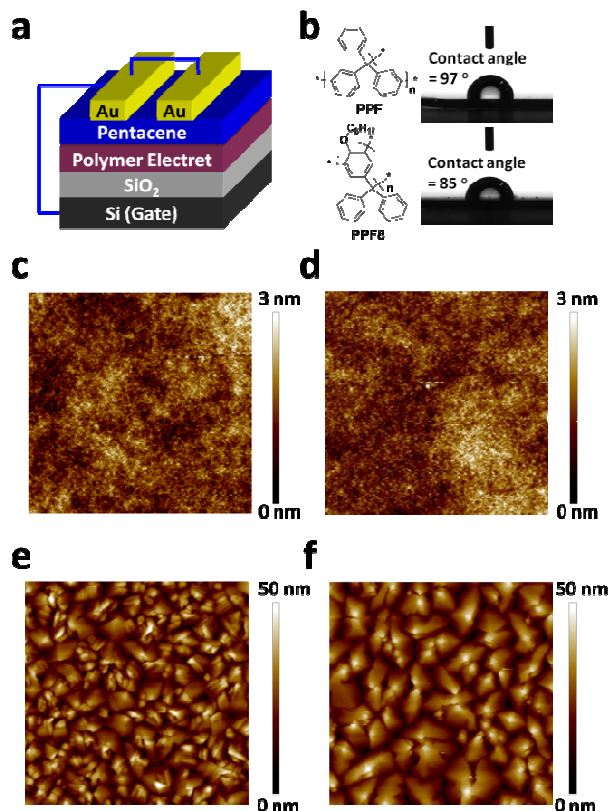

Figure 2. (a) Schematic configuration of the transistor memory device, (b) Molecular structures of PPF and PPF8, and contact angles of films surface: spin-coated from toluene onto SiO$_2$ (side view of a drop of water). AFM topographic images of (c) PPF8, (d) PPF films and pentacene on different surfaces: (e) PPF8, (f) PPF modified SiO$_2$ surface on 5 × 5 μm.

Morphology and Electrical Characterization of Transistor Memory Devices. Figure 2a presents the schematic diagram of prototype pentacene-based transistor memories based on a bottom-gate top-contact configuration, in which PPF and PPF8 are used as the chargeable polymer electrets. The film thicknesses of each layer are determined to be approximately 60 nm of PPF and PPF8, 50 nm of pentacene and 25.5 nm of Au source/drain electrodes. The representative contact angles of the SiO$_2$/PPF or PPF8 bilayer film are shown in Figure 2b. The hydrophobic characteristic of the PPF and PPF8 with a water contact angle of 97 °(15.29 mN/m) and 85 °(22.40 mN/m) ensures good wetting and the well-formed growth of pentacene on the smooth electret surface.[30] On this regard, the alkoxyl substitution may increase the hydrophilic properties and surface energy, which further effected on the growth and crystallinity of pentacene. Comparatively, the water contact angle of clean and bare SiO$_2$ is 53 °. These indicate that the surface energy of PPF and PPF8 is lower compared to that of a bare SiO$_2$ surface, which further effect on the morphology of pentacene.

The surface morphology of PPF and PPF8 are shown in Figure 2c and 2d. The film structure of the polymer electrets through conventional solution spin-coating process on bare SiO$_2$ substrates exhibit smooth surface with small root-mean-square values of 0.2-0.3 nm (Figure 2c, 2d and S5), but exhibit amorphous phase according to out-of-plane X-ray diffraction (Figure S6). The representative AFM images of pentacene on polymer electrets are also shown in Figure 2e and 2f. The grain sizes of pentacene grown on the PPF8 and PPF surface are 0.21 and 0.93 μm, suggested larger grain size of pentacene grown on the PPF than those on PPF8 for lower surface energy and polarity. The flexible alkoxyl substitution would result into disorder molecular aggregation on the nano-surface of PPF8 film, which may lead to less ordered packing in the deposited pentacene layer.[43] Out-of-plane X-ray diffraction profiles of the pentacene thin films deposited on the PPF with a d-spacings of 15.4 Å exhibit stronger diffraction intensity and a narrower full width at half maximum than those of pentacene film on the PPF8 surface (d-spacings = 15.7 Å) (Figure S7). These evidences support the premise that PPF layer will improve the intermolecular transfer integral and the crystalline structures of the pentacene than those on PPF8. And the vacuum-deposited pentacene films was exhibited thin-film phase, which the corresponding device of the thin-film phase exhibit relatively larger mobility in contrast to the small bulk-phase crystallites.
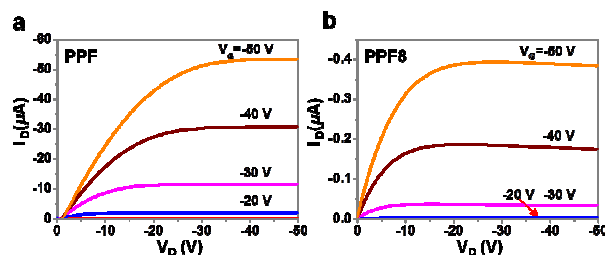
Figure 3. Output characteristics of transistor memory devices with (a) PPF and (b) PPF8 as the polymer electret.

The electrical output and transfer characteristics of the devices are shown in Figure 3 and S8. These curves exhibit typical p-type field - effect transistor behaviour. The V-shape transfer curves show good current modulation and the output curves exhibit well defined linear and saturation regions. From figure 3 and S8, the field-effect mobility of PPF-based device in the saturation region would comparable to those analogous traditional polymers electrets,[31] and exhibit higher than device based on PPF8, for PPF and PPF8 at the source to drain voltage (V$_D$) of -30 V. The threshold voltage (V$_{th}$) and the I$_{on}$/I$_{off}$ current ratio of PPF and PPF8 were about -14.3, -20.8 V and 10^5, 10^4, respectively. The higher field-effect mobility and larger I$_{on}$/I$_{off}$ current ratio are observed from the devices with PPF as polymer electret compared to PPF8, which may be due to the morphology of pentacene on PPF8, that the pentacene exhibits smaller grain size and many grain boundaries, leading to a reduction of hole mobilities, corresponding to the results of AFM analysis. On the other hand, the I$_{on}$/I$_{off}$ is significantly affected by both the charge transport ability of active layer and leakage current of the dielectric layer, which are significantly associated to polar and hydrophobic property of polymer electrets.
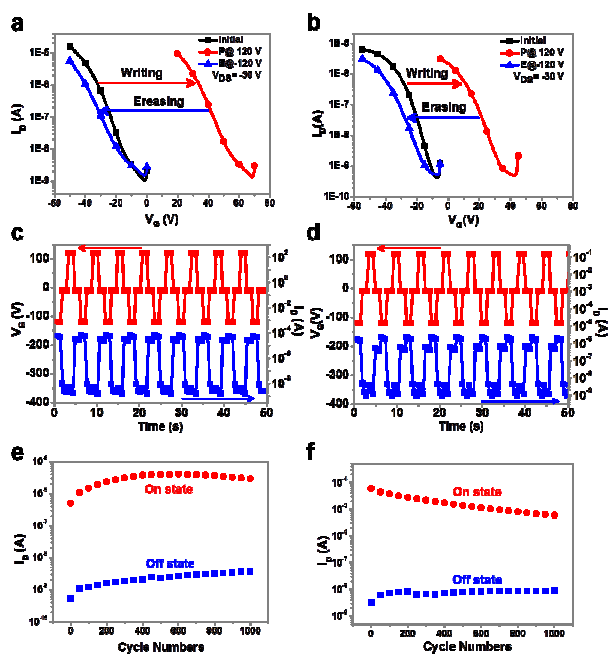
Figure 4. Reversible shifts in V_{th}, reversible switching for ON- and OFF- states, and WRER cycle testing of transistor memory device with (a, c, e) PPF and (b, d, f) PPF8 as polymer electret, respectively. The drain current was measured at V_D = -30 V. The writing, reading, and erasing were at the gate voltages of -120, 0, and +120 V, respectively.

Pentacene-based Transistor Memory Performance. The pentacene-based transistor memory device operated by applied appropriate gate pulse (+/-120 V)，which led to the shifts of transfer curves, causing the high- (ON) and low-conductance (OFF) states. Figure 4 shows the shifts in transfer curve for the pentacene-based transistor memory devices with PPF and PPF8 as polymer electrets. The drain current was kept at V_{DS} =-30 V. When applied a positive gate bias (V_G =120 V for 1 s), the transfer curves using PPF, PPF8 were substantially shifted in the positive direction with threshold voltages of 70 V and 42 V, respectively, serving as the ''writing'' process. The shifts led to a high drain current (ON state) at V_g =0 V. When applied a reverse gate bias (V_G =-120 V for 1 s), the transfer curves were shifted to negative direction for PPF, PPF8 with threshold voltages of -2 and -7.5 V, respectively, which was denoted as the ''erasing'' process. Meanwhile, the drain current at V_G = 0 V was dramatically reduced, and the devices were returned to the low conductance (OFF state). Memory window, which is defined as the amount of shift in the V_{th} on the application of different gate bias, was 72 V and 49.5 V for PPF and PPF8, respectively (Figure S9). The multiple switching stability of the device using PPF and PPF8 as electrets was evaluated through write-read-erase-read (WRER) cycles, as shown in Figure 4c and 4d. The operation conditions of WRER cycles are summarized as follows. The drain current was measured at V_{DS} =-30 V. The writing, reading and erasing processes were conducted at the gate voltages of -120 V, 0, and +120 V, respectively. The devices exhibited excellent memory characteristics with high ON/OFF current ratios (~10^3). The responding ON and OFF currents of the devices are maintained over 1000 cycles with a high ON/OFF

current ratio of 10^3 (Figure 4e and 4f), which reveals the promising potential applications for nonvolatile transistor memory devices. The time during which the stored charge is retained in the dielectric layer, is defined as the retention time. Figure 5 are the retention time of the pentacene thin film with PPF or PPF8 as electrets. The retention time of the ON and OFF states of the device at a gate voltage of 0 V is maintained for 10^4 s with a high on/off current ratio of around 10^3. This long retention time indicates that the CIHPs are promising polymer electrets for reliable and stable organic nonvolatile memories. The good memory stability and reversibility reveal that the transistor memories with CIHPs electrets via precise molecular design have excellent potential for the applications of nonvolatile flash-type memories. However, for the substitution of alkoxyl groups, the transistor memory device based on PPF8 showed lower memory stability than PPF-based devices.
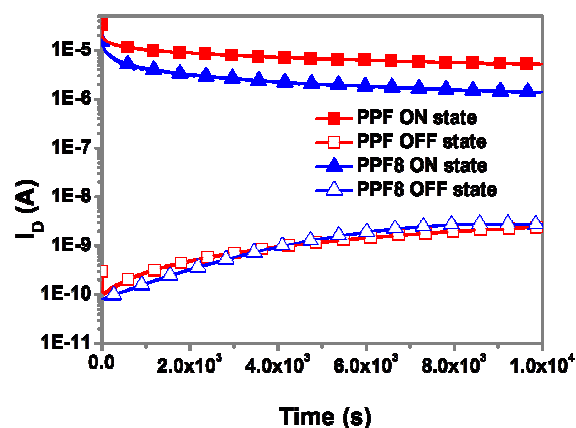
Figure 5. Retention characteristics of transistor memory devices with PPF and PPF8 as the polymer electret.

The promising mechanism are proposed in Figure S10.[31] When the device is subjected to a high positive V_G for programming, the electrons inject from the LUMO of pentacene into the unoccupied states of the PPF and PPF8 film, followed the Fowler-Nordheim (FN) tunnelling as the dominant mechanism. The positive charges can be induced in the pentacene after programming process, bringing about the positive shift of V_{th} for the ON state. While the injection of holes from pentacene to PPF and PPF8 film neutralize the previously trapped electrons during erasing as the large negative V_G applied, and subsequently result in the free charge of pentacene which switches the device from ON state to OFF state. PPF possesses the smaller LUMO energy barrier (0.81 eV) compared to PPF8 (0.96 eV), thus facilitating the electrons transfer from pentacene to PPF and leading to a larger positive shift in the threshold voltage (70 Vs 42 V). For the erasing process, the trapped charges in the polymer electrets are detrapped by applying a high negative gate voltage. The erasing process may occur through hole injection from pentacene induced by the negative gate voltage, leading to the recombination with electrons trapped in polymer electrets, as shown in Fig. S10b. In this context, PPF8 possesses the smaller HOMO energy barrier (0.89 eV), thus leading to the larger negative shift in the threshold voltage (7.5 Vs 2 V).

It is easy to come to conclude that the performance of transistor memory device was significantly associated with structure dimension, molecular aggregation behaviour, substitution unit, polarity and film morphology of polymer electrets. The chain rigidity of PPF is restricted by the central fluorene core, which forms a higher fluorene trapping density and molecular aggregation than those of PPF8 in film states (Figure 2).[11, 23] Meanwhile, the 3-D fluorene structure of PPF exhibited stronger steric hindrance effects at nano-interface, which would improve charge mobility and memory window of transistor memory devices for the more charge trapping sites.[37] The larger grain sizes and crystalline of pentacene grown on the PPF would attribute to its lower surface energy, hydrophobic and non-polar properties. The negative or positive shift on the threshold voltage may dominate by the energy barrier between pentacene and polymer electrets. The alkoxyl substitution would increase the energy level and hydrophilic properties, and further decrease crystallinity and grain size of pentacene. In addition, better performance and stability of PPF-based transistor memory device than those based on PPF8 indicated the substitution of alkoxyl groups have a negative impact on the performance and stability of transistor devices. Soluble organic nanoframeworks will be potential advanced organic materials in organic molecular and nanoscale electronics as well as mechatronics.

Conclusion

In conclusion, we make a rational molecular design of polymer electrets based on pi-conjugation-interrupted organic frameworks for the application of transistor memory devices. Fluorene-based CIHPs have been synthesized successfully via atom-economic F-C C-H bond polymerization. They exhibited excellent thermal stability solubility and film-forming ability. The transistor memory device based on the PPF as electrets exhibited the higher mobility than those of PPF8-based devices. This is attributed to the larger grain sizes and crystalline of pentacene on the polymer films, resulted from lower surface energy, hydrophobic and non-polar properties of PPF. PPF-based devices also exhibit the larger memory window and better stability compared to those of PPF8, indicating that the substitution of alkyl groups worsen transistor memory device performances. Nevertheless, the intrinsic 3-dimensional topological network, potential nanoporous structures and interrupted conjugation length make CIHPs serve as polymer electrets. CIHPs will be one kind of excellent candidate materials as polymer electrets via four-element molecular design in the transistor memory devices.

Acknowledgments

Notes and references

aCenter for Molecular Systems and Organic Devices (CMSOD), Key Laboratory for Organic Electronics & Information Displays (KLOEID), Institute of Advanced Materials (IAM), Nanjing University of Posts and Telecommunications, Nanjing, P. R.. China. Fax: +86 025 8586 6396; E-mail: (L.X.) iamlhxie@njupt.edu.cn; (W.H.) iamwhuang@njupt.edu.cn; (M.Y.) iammdyi@njupt.edu.cn;
bDepartment of Chemistry, Central China Normal University, Wuhan Hubei, 430079, P. R. China
c Jiangsu-Singapore Joint Research Center for Organic/Bio Electronics & Information Displays, Institute of Advanced Materials, Nanjing Tech University, Nanjing 211816, China.
† Electronic Supplementary Information (ESI) available: Full experimental section, including detailed synthesis of monomer and polymer, NMR analysis; DSC and DTG curve; cyclic voltammetry (CV) study; absorption and PL spectra; SEM image; XRD data; device performance. See DOI: 10.1039/b000000x/

1.   S. Möller, C. Perlov, W. Jackson, C. Taussig and S. R. Forrest, Nature 2003, **426**, 166.
2.   L.-H. Xie, C.-R. Yin, W.-Y. Lai, Q.-L. Fan and W. Huang, *Prog. Polym. Sci.*, 2012, **37**, 1192.
3.   P. Heremans, G. H. Gelinck, R. Muller, K.-J. Baeg, D.-Y. Kim and Y.-Y. Noh, *Chem. Mater.*, 2010, **23**, 341.
4.   L.-H. Xie, Q.-D. Ling, X.-Y. Hou and W. Huang, *J. Am. Chem. Soc.*, 2008, **130**, 2120.
5.   J. Liu, Z. Yin, X. Cao, F. Zhao, A. Lin, L. Xie, Q. Fan, F. Boey, H. Zhang and W. Huang, *ACS Nano*, 2010, **4**, 3987.
6.   J. Liu, Z. Lin, T. Liu, Z. Yin, X. Zhou, S. Chen, L. Xie, F. Boey, H. Zhang and W. Huang, *Small*, 2010, **6**, 1536.
7.   C.-R. Yin, Y. Han, L. Li, S.-H. Ye, W.-W. Mao, M.-D. Yi, H.-F. Ling, L.-H. Xie, G.-W. Zhang and W. Huang, *Polym. Chem.*, 2013, **4**, 2540.
8.   P. Wang, S.-J. Liu, Z.-H. Lin, X.-C. Dong, Q. Zhao, W.-P. Lin, M.-D. Yi, S.-H. Ye, C.-X. Zhu and W. Huang, *J. Mater. Chem.*, 2012, **22**, 9576.
9.   F. Zhao, J. Liu, X. Huang, X. Zou, G. Lu, P. Sun, S. Wu, W. Ai, M. Yi, X. Qi, L. Xie, J. Wang, H. Zhang and W. Huang, *ACS Nano*, 2012, **6**, 3027.
10.   T. Sekitani, T. Yokota, U. Zschieschang, H. Klauk, S. Bauer, K. Takeuchi, M. Takamiya, T. Sakurai and T. Someya, *Science*, 2009, **326**, 1516.
11.   L. Zhang, T. Wu, Y. Guo, Y. Zhao, X. Sun, Y. Wen, G. Yu and Y. Liu, *Sci. Rep.* 2013, **3**, DOI: 10.1038/srep01080.
12.   S.-J. Kim and J.-S. Lee, *Nano Lett.*, 2010, **10**, 2884.
13.   S. Park, G. Wang, B. Cho, Y. Kim, S. Song, Y. Ji, M.-H. Yoon and T. Lee, *Nat. Nanotechnol.*, 2012, **7**, 438.
14.   Y. Guo, C.-a. Di, S. Ye, X. Sun, J. Zheng, Y. Wen, W. Wu, G. Yu and Y. Liu, *Adv. Mater.*, 2009, **21**, 1954.
15.   Y. Guo, G. Yu and Y. Liu, *Adv. Mater.*, 2009, **22**, 4427-4447.
16.   Y.-H. Chou, W.-Y. Lee and W.-C. Chen, *Adv. Funct. Mater.*, 2012, **22**, 4352.
17.   B. Liu, M. A. McCarthy and A. G. Rinzler, *Adv. Funct. Mater.*, 2010, **20**, 3440.
18.   P. Stadler, K. Oppelt, T. B. Singh, J. G. Grote, R. Schwödiauer, S. Bauer, H. Piglmayer-Brezina, D. Bäuerle and N. S. Sariciftci, *Org. Electron.*, 2007, **8**, 648.
19.   T.-W. Kim, Y. Gao, O. Acton, H.-L. Yip, H. Ma, H. Chen and A. K. Y. Jen, *Appl. Phys. Lett.*, 2010, **97**, 023310.
20.   J. Ouyang, C.-W. Chu, C. R. Szmanda, L. Ma and Y. Yang, *Nat Mater*, 2004, **3**, 918.
21.   K.-J. Baeg, Y.-Y. Noh, H. Sirringhaus and D.-Y. Kim, *Adv. Funct. Mater.*, 2010, **20**, 224.
22.   L. A. Majewski, R. Schroeder and M. Grell, *Adv. Mater.*, 2005, **17**, 192.

23. Y.-C. Chiu, C.-L. Liu, W.-Y. Lee, Y. Chen, T. Kakuchi and W.-C. Chen, *NPG Asia Mater*, 2013, **5**, e35.

24. T. T. Dao, T. Matsushima and H. Murata, *Org. Electron.*, 2012, **13**, 2709.

25. K. J. Baeg, Y. Y. Noh, J. Ghim, S. J. Kang, H. Lee and D. Y. Kim, *Adv. Mater.*, 2006, **18**, 3179.

26. M. Kang, K.-J. Baeg, D. Khim, Y.-Y. Noh and D.-Y. Kim, *Adv. Funct. Mater.*, 2013, **23**, 3503.

27. R. C. G. Naber, C. Tanase, P. W. M. Blom, G. H. Gelinck, A. W. Marsman, F. J. Touwslager, S. Setayesh and D. M. de Leeuw, *Nat Mater*, 2005, **4**, 243.

28. R. C. G. Naber, K. Asadi, P. W. M. Blom, D. M. de Leeuw and B. de Boer, *Adv. Mater.*, 2010, **22**, 933.

29. Y.-H. Chou, N.-H. You, T. Kurosawa, W.-Y. Lee, T. Higashihara, M. Ueda and W.-C. Chen, *Macromolecules*, 2012, **45**, 6946.

30. K.-J. Baeg, Y.-Y. Noh, J. Ghim, B. Lim and D.-Y. Kim, *Adv. Funct. Mater.*, 2008, **18**, 3678.

31. J.-C. Hsu, W.-Y. Lee, H.-C. Wu, K. Sugiyama, A. Hirao and W.-C. Chen, *J. Mater. Chem.*, 2012, **22**, 5820.

32. Y.-C. Chiu, T.-Y. Chen, C.-C. Chueh, H.-Y. Chang, K. Sugiyama, Y.-J. Sheng, A. Hirao and W.-C. Chen, *J. Mater. Chem. C.* 2014, DOI: 10.1039/c3tc31840k.

33. C. Kim, A. Facchetti, T. J. Marks, Science 2007, **318**, 76-80.

34. A.-D. Yu, T. Kurosawa, M. Ueda and W.-C. Chen, *J. Polym. Sci. Part A: Polym. Chem.* **2014**, 52, 139.

35. J.-C. Hsu, Y. Chen, T. Kakuchi and W.-C. Chen, *Macromolecules*, 2011, **44**, 5168.

36. Y.-H. Chou, S. Takasugi, R. Goseki, T. Ishizone and W.-C. Chen, *Polym. Chem.* 2014, **5**, 1063.

37. M.-H. Jung, K. H. Song, K. C. Ko, J. Y. Lee and H. Lee, *J. Mater. Chem.*, **20**, 8016.

38. L.-H. Xie, Y. Z. Chang, J. F. Gu, R. J. Sun, J. W. Li, X. H. Zhao, W. Huang, *Acta Phys.-Chim. Sin.* 2010, **26**, 1784.

39. L.-H. Xie, X.-Y. Hou, Y.-R. Hua, C. Tang, F. Liu, Q.-L. Fan and W. Huang, *Org. Lett.*, 2006, **8**, 3701.

40. L.-H. Xie, X.-Y. Deng, L. Chen, S.-F. Chen, R.-R. Liu, X.-Y. Hou, K.-Y. Wong, Q.-D. Ling and W. Huang, *J. Polym. Sci. Part A: Polym. Chem.*, 2009, **47**, 5221.

41. Y. Z. Chang, Q. Shao, L.-Y. Bai, C.-J. Ou, J.-Y. Lin, L.-H. Xie, Z.-D. Liu, X. Chen, G.-W. Zhang, W. Huang, *Small* 2013, **9**, 3218.

42. Z.-D. Liu, Y.-Z. Chang, C.-J. Ou, J.-Y. Lin, L.-H. Xie, C.-R. Yin, M.-D. Yi, Y. Qian, N.-E. Shi and W. Huang, *Polym. Chem.*, 2010, **2**, 2179.

43. H. S. Lee, D. H. Kim, J. H. Cho, M. Hwang, Y. Jang and K. Cho, *J. Am. Chem. Soc.*, 2008, **130**, 10556.